

The histopathology of *Candida albicans* invasion in neonatal rat tissues and in the human blood-brain barrier in culture revealed by light, scanning, transmission and immunoelectron microscopy

A.S. Lossinsky¹, A. Jong², M. Fiala³, M. Mukhtar⁴, K.F. Buttle⁵ and M. Ingram⁶

¹Immunohistochemistry and Electron Microscopy Laboratories, Neural Engineering Program, Huntington Medical Research Institutes, Pasadena, California,

²Department of Pediatrics, Children's Hospital of Los Angeles and the USC School of Medicine, Los Angeles, CA,

³Department of Medicine and Oral Biology, UCLA School of Medicine, Los Angeles, CA,

⁴Division of Infectious Diseases, Thomas Jefferson University School of Medicine, Philadelphia, PA,

⁵Resource for Visualization of Biological Complexities, Wadsworth Center, Albany, NY, and

⁶Department of In Vitro Systems and Tissue Engineering, Huntington Medical Research Institutes, Pasadena, California.

Summary. The present studies examined the effects of *Candida albicans* yeast and hyphal morphologies on tissue pathologies and transmigration properties of the fungus in two experimental models: 1) an *in vivo*, neonatal rat model, and 2) a cell culture model of human brain microvascular endothelial cells (ECs) (BMVEC). We inoculated a hyphae-producing strain (CAI4-URA3) and a non-hyphae-producing strain (CAI4) of *C. albicans* into 4-10 day old rats and BMVEC cultures. Animals were inoculated by intraperitoneal (i.p.), intranasal (i.n.), oral (p.o.) and intracerebral (i.c.) routes and several tissues were examined after 24-48 hrs. Rats inoculated i.p. with the hyphae-producing strain showed pathology in the kidneys, liver, spleen, and other tissues associated with inoculation tracks of the nose, and muscle and connective tissues of the abdominal wall. Few animals inoculated i.p., however, presented evidence of meningitis. The non-hyphae phase yeast produced neither tissue pathology nor meningitis. Animals inoculated i.c. with the hyphae strain after 1 and 3 hrs expressed minimal meningitis, with an increasing neutrophilic meningitis between 4 and 18 hrs after inoculation. At 18 hrs after i.c. inoculation, however, the inflammatory foci and brain pathology were extensive and demonstrated mycelia within the lateral ventricles associated with necrosis of adjacent brain tissue. Neutrophilic meningitis at this time period

was pronounced. BMVEC co-cultured 1-2 hrs with both *C. albicans* strains showed EC phagocytosis of hyphae and blastospores into intercellular adhesion molecule-1 (ICAM-1)-labeled caveolae suggesting a transcellular role for ICAM-1 in the internalization process of *C. albicans*.

Key words: *Candida albicans*, Blood-brain barrier

Introduction

Candida albicans belongs to a group of pathogenic microorganisms that produce meningitis in neonates and adults (Davis and Rudd, 1994; Witek-Janusek et al., 2002). The microorganism accomplishes this by presenting a battery of putative virulence factors that often overcome the weakened host defense (Naglik et al., 2003). *C. albicans* is thought to be contracted from the mother during natural birth (Davis and Rudd, 1994). The fungus likely enters the mucous membranes of the eyes and nose. In premature infants, meningitis can occur after the organism enters the blood stream via central venous and other line catheters (Holler et al., 2004). The infant also swallows the fungus during the birthing process that promotes the gastric fungal burden (Witek-Janusek et al., 2002). *Candida* infections of the brain arise via hematogenous seeding in the vast majority of cases (Chimelli and Mahler-Araujo, 1997).

Although the pathology of tissue Candidiasis and *Candida* meningitis and its clinical ramifications have been well documented in newborn and adult humans, there is limited available literature that defines the

precise mechanisms of transmigration of this pathogen to the brain across the restrictive vasculature of the CNS, i.e., the blood-brain barrier (BBB). Previous studies employing models of cultured endothelial cells (ECs), in both BBB-type (Jong et al., 2001), and in non-BBB-type in human umbilical cord ECs (HUVEC, Filler et al., 1995, 1996) and in bovine aortic ECs (Zink et al., 1996), demonstrated that *C. albicans* penetrates the EC barriers using a transcellular rather than junctional route for its invasion of the ECs. However, understanding the specific mechanism(s) of transmigration of this pathogen and the leukocytes that respond to the invasion of the BBB in both living animals and in culture systems have not been fully delineated.

Here we applied several morphologic and immunohistochemical approaches to further investigate how *C. albicans* invades and traverses the BBB. We questioned whether *C. albicans* follows a penetration pathway across the BBB similar to that followed by macromolecules, as well as inflammatory and neoplastic cells (reviewed in Lossinsky and Shivers, 2004). Our studies tested the development of meningitis in newborn rats using several inoculation pathways of *C. albicans* including nasal, oral, intraperitoneal and intracerebral routes. Moreover, we evaluated of the nature of transmigration of both hyphae-producing and non-hyphae-producing strains of the fungus in a cell culture system of human BMVEC. We examined whether this pathogen utilizes a transcellular, cytoplasmic route, or a paracellular pathway via EC junctional complexes. Our data suggest a rodent model for neonatal meningitis complemented with an *in vitro* model of the human BBB and also imply a strong role for ICAM-1 in *C. albicans* invasion of the BBB.

Materials and methods

Culture conditions for C. albicans

In these studies, we compared hyphal and non-hyphal strains of *C. albicans*. We used: 1) a strain that produces hyphae and causes tissue pathology in animals because it contains uracil = Δ CAI4-URA), Δ ura3::imm434/ Δ ura3::imm434:: Δ URA3;), provided by Dr. Scott Filler, Harbor-UCLA Medical Center, Torrance, CA, and 2) a non-hyphal producing strain that remains in the cellular phase and does not produce tissue pathology (CAI4 = Δ ura3::imm434/ Δ ura3::imm434) provided by Dr. Ambrose Jong, CHLA, Los Angeles, CA). Both forms of the fungus were grown in YPD medium at 30°C on a rotary shaker overnight, centrifuged, washed X2 with sterile phosphate buffered saline (PBS), resuspended in YPD medium and counted with a hemocytometer prior to inoculations into both neonatal rats and BMVEC cultures at 37°C.

Neonatal rats

The procedures using neonatal rats conform to the

National Institute of Health's guidelines for animal care and handling and were approved by the Institute's Animal Care and Use Committee of the Huntington Medical Research Institutes. Timed pregnant, young female Sprague Dawley rats were purchased from Harlan Co. (San Diego, CA) and arrived at the animal facility on the 14th day of pregnancy, (E₁₄). The animals remained in quarantine for at least 1 week after which the mothers delivered their young, usually 12-14 pups/litter. These animals remained undisturbed, usually at least 10 days prior to selection of the rat pups for each experiment.

Anesthesia, rat inoculations

Rat pups subjected to the various routes of inoculation were anesthetized by first placing them into a latex glove and totally submerging them in an ice slush bath for 3-4 min. to produce hypothermia (Baer, 2004). Rats were given either strain of *C. albicans*, usually 10⁶-10⁷ yeast cells in 0.1 ml PBS via intraperitoneal inoculations (i.p.), intranasal injections (i.n.), oral (p.o.) and intracerebral (i.c.) routes. The rats inoculated by i.p., i.n. and p.o. were examined after 24 and 48 hrs. Animals inoculated by the i.c. route were sacrificed after 1, 3, 4, 4.5, and 18 hrs post inoculation. Rat pups surviving longer i.p., i.n. and p.o. inoculation periods (18-48 hrs) were returned to their mothers. In short term animal experiments (1-4.5 hrs), rat pups were maintained on a heated water bed with an overhead heating lamp at 35-37°C, and not returned to the mother's cages before they were selected for vascular perfusion. All animals regained their normal pink color and activity after several minutes on the heated waterbeds. Rats were euthanized using a single i.p. injection of 0.1 ml sodium pentobarbital (50 mg/ml).

Growth and propagation of human BMVEC.

BMVEC were purified from discarded temporal lobe tissue obtained after Institutional Review Board approval and informed consent from lobectomized, epileptic patients from the University of Arizona, Tucson, AZ. These were grown to confluence on sterile 16mm diameter Nalgene cover slips with in sterile 24-well plastic dishes (Falcon Plates, Becton Dickinson & Co., Lincoln Park, NJ, USA), according to our previous report (Liu et al., 2002). The BMVEC were maintained on DMEM-F12 medium containing 10% fetal bovine serum and penicillin and streptomycin. After the desired time of yeast co-cultivation, the coverslips were washed and fixed according to the specific scheduled experiment.

Methods of inoculation of C. albicans into BMVEC

Although the CAI4 strain does not produce tissue pathology by virtue of the fact that it does not produce hyphae, we wanted to establish whether or not

C. albicans histopathology and the BBB

adhesion/invasion of BMVEC differ in the two yeast strains. Thus, we inoculated confluent BMVEC cultures with both strains of *C. albicans* grown on cover slips in culture plates using sterile PBS containing 10^6 - 0.5×10^7 yeast cells/well. In all our experiments, we examined BMVEC cultures at 1 and 2 hrs after inoculation.

Vascular perfusion of neonatal rats for light microscopy (LM), immunohistochemistry and high-voltage electron microscopy (HVEM) studies

We used a dissecting microscope during transcatheter perfusion of all neonatal rat pups according to previously described methods (Lossinsky et al., 1986). Briefly, after euthanasia, the chest wall was opened and the apex of the heart was cut. A cannula made from a 27 GA, blunt-tipped metal needle was then inserted into the left cardiac ventricle and held in its position using a small mosquito hemostat. The animals were flushed with 5 ml PBS solution containing heparin (10 units/ml) and 0.01% procaine hydrochloride to wash away the blood. This prewash solution was immediately followed by 50 ml of: 1) 4% formalin solution (freshly prepared from paraformaldehyde powder) in 0.1 M sodium cacodylate buffer at 25°C, pH 7.4 (Lossinsky et al., 1999) for light microscopy (LM) studies, and 2) 1/2 strength Karnovsky's Fixative (1/2 K, Karnovsky, 1965) prepared with 3% glutaraldehyde, 2% formalin (freshly prepared from paraformaldehyde powder) in 0.1 M sodium phosphate buffer at 25°C, pH 7.4 for HVEM studies. We used a hydrostatic drip method (Kalimo et al., 1974) to perfuse all neonatal rats. After fixation, kidneys, livers, spleens, lungs, brains and tissues from the nose and abdominal muscles in the vicinity of the inoculation channel were dissected and immersed in the above LM fixative. Coronal brain slabs (2-3 mm) containing the inoculation channels were removed and immersed with the other tissues in the above-mentioned LM fixative overnight in the refrigerator at ca. 5-8°C. Rat brains (perfused with 1/2 K fixative) that contained inoculation tracks and/or brain regions showing gross trauma were selected for HVEM studies. Afterwards, all tissues to be used for LM were washed with 0.1 M phosphate buffer. HVEM samples were held until further processing in a buffer containing 0.2 M sucrose and 0.1 M sodium cacodylate with 0.01% sodium azide (S/C buffer) at 5-8°C. LM tissues were embedded in paraffin and cut at 5-8 µm sections. Brain tissues scheduled for HVEM analyses were post-fixed with osmium tetroxide and embedded in plastics as described below.

Immunohistochemistry was performed on unstained kidney sections. After vascular perfusion, these 5-8 µm sections were picked up on Histogrip-coated glass slides. Endogenous peroxidase activity was blocked with 1% H₂O₂ in absolute methanol. For antigen retrieval, the sections were then microwaved (70% power, 800 watts 3 min X4) adjusting the level of the citrate buffer, enzyme digested with DAKO proteinase K, blocked with Zymed non-immune serum blocking solution according to a

previously described method (Shi et al., 1991). We used mouse monoclonal anti-human *C. albicans* (1:100 dilution) incubated at 25°C for 1 hr. We used a biotinylated polyclonal goat anti-mouse IgG, H+L (1:50 dilution) incubated at 25°C for 1 hr., washed with PBS 6X between antibody incubations and labeled with avidin-peroxidase. The negative control groups used incubation systems in which the primary antibodies were omitted. After several PBS washes, all LM histologic and immuno-histochemistry sections were lightly counterstained with hematoxylin or Nissl stains. These antibodies and other reagents were purchased from Chemicon Corp., Temecula, CA, and other immunology reagent suppliers (Linscott, 1999).

Transmission electron microscopy (TEM), immunostudies using a pre-embedding incubation procedure

The preembedding method was selected such that membrane antigenic epitopes can be recognized in fixed tissues prior to post-fixation with osmium tetroxide (Lossinsky and Shivers, 2003). We fixed BMVEC cultures with either a 4% solution of formalin, or 4% formalin containing 0.1-0.25% glutaraldehyde, as described above (Lossinsky et al., 1999). The BMVECs were quenched with 1% NH₄Cl for 20 min at 25°C in a shaker-water bath to remove unbound aldehyde groups and treated with 1% H₂O₂ in PBS for 30 min at 25°C to remove endogenous peroxidase activity. The cells were blocked with 10% goat serum in PBS (PBSS) overnight at 4° C. Each incubation vial contained the tissue samples and a total volume of 250µl, including antibodies, PBSS and immunoperoxidase probe. Primary antibody (mouse anti-human monoclonal antibody prepared against intercellular adhesion molecule-1 (ICAM-1) was diluted at 1:100 dilution in PBSS. Incubations were carried out overnight at 4°C. After incubations, the tissues were washed 8X with PBSS to insure removal of unbound antibody. The secondary antibody was biotinylated goat anti-mouse IgG diluted 1:50 with PBSS. Incubation with secondary antibodies was at 25°C for 1 hr with gentle rotation. After washing 8X with PBSS, the BMVEC were incubated in a 1:50 dilution of ExtrAvidin-peroxidase at 25°C for 1-1.5 hrs. After washing 4X with PBS, the tissue was reacted with 3,3'-diaminobenzidine tetra-HCL (DAB) to localize specific peroxidase activity (Liu et al., 2002). Immunoreagents were purchased from Accurate Chemical & Scientific Corp., San Diego, CA, and Chemicon Inc, Temecula, CA. Extravidin-peroxidase probe was purchased from Sigma Chemical Co., St Louis, MO (Linscott, 1999).

BMVEC cultures, TEM and HVEM studies

BMVEC cultures grown on cover slips in 24-well plastic dishes were fixed by immersion according to standard protocols, taking into consideration our desire

C. albicans histopathology and the BBB

to produce excellent ultrastructural preservation of EC cytoskeletal filaments, microtubules, and EC junctional complexes. For this reason, we fixed the BMVEC at room temperature (25°C) to avoid disruption of EC cytoskeletal components such as microtubules. The fixative contained 2.5-3.0% glutaraldehyde in 0.1 M sodium cacodylate buffer, pH 7.4 (Haudenschild et al., 1975). BMVEC were post-fixed with 1% osmium tetroxide, dehydrated in a graded series of ethanol, and *en bloc* stained with uranyl acetate (Hayat, 1981). The coverslips were infiltrated with liquid epoxy plastic overnight in a desiccator at 25°C. On the next day, in liquid plastic, the coverslips were sliced into several pieces and flat-embedded with the BMVEC positioned upward, then polymerized in a 60°C oven overnight. For TEM and HVEM studies, plastic thick- and thin-sections were cut with either the Leica Ultracut UCT and Sorvall (MT-1) Ultramicrotomes and stained with lead and uranyl salts, according to standard protocols (Hayat, 1981). TEM was performed with the FEI Morgagni Electron Microscope. For thin-section studies, grids were stained with uranium and lead salts. For HVEM studies, 0.25-1.0µm serial-thick sections were collected on 1% formvar-coated slot grids (Lossinsky et al., 1989b). Staining in 2% uranyl acetate was at 50°C for 1.5 hr and at 25°C for 30 min in lead citrate. Stereo-pair micrographs were taken at 1,000 kV using the AEI EM7 High-Voltage Electron Microscope at the Resource for Visualization of Biological Complexities, Wadsworth Center, (Albany, NY) (Lossinsky et al., 1989b; Lossinsky and Shivers, 2003).

Scanning electron microscopy (SEM), BMVEC

Plastic coverslips containing BMVEC were fixed as described above for TEM and HVEM studies, post-fixed with 1% OsO₄ in S/C buffer, washed in S/C buffer overnight at 4°C and subsequently dehydrated in a graded series of ethanol. BMVEC cultures in absolute ethanol were chemically dried using hexamethyldisilazane (Bray et al., 1993; Lossinsky and Shivers, 2003). The dried cover slips were glued to aluminum SEM stubs, shadow coated with gold/palladium vapor using a Pelco SC-7 Sputter Coater and scanned with a FEI XL30 ESEM (Lossinsky and Shivers, 2003).

Results*Light microscopy and immunohistochemistry, neonatal rats inoculated with CAI4-URA*

To determine the nature of tissue pathology and meningitis produced by the hyphae-phase strain of *C. albicans*, 4-10 day post partum rats were subjected to i.p. inoculations of *C. albicans* CAI4-URA. Table 1 summarizes the methods of inoculations used and the times after infection in these *in vivo* studies. Meningitis was produced via the i.p. route, although this strain did not cause detectable tissue pathology when administered by mouth or nasal routes. Kidney cortical and medullary portions contained mycelia with mixed leukocytes, but invasion of the glomeruli was not observed (Fig. 1a, b). We observed minimal presence of hyphae within the

Table 1.

Exp. No.	Rats/group, Inoculation Routes	Neonatal Age (days)	Candida Strain	Method, Time After Inoculation	Histopathology	Meningitis
1	4 - p.o 4 - i.n. 4 - i.p. 2 - Neg. controls	5	CAI4-URA	24-48 hr	negative	0/12
2	11 - i.p. 2 - Neg. controls	4	CAI4-URA	36, 40 hr	l, k, s	3/11 +/-
3	11 - i.p. 2 - Neg. controls	10	CAI4-URA	44-48 hr	l, k, s	1/11 +/-
4	8 - i.c. 2 - Neg. controls	6	CAI4-URA	1, 3 hr	l, k, s	1/8 +/-
5	8 - i.c. 2 - Neg. controls	6	CAI4-URA	4-18 hr	np	8/8 +++
6	8 - i.c. 2 - Neg. controls	6	CAI4-URA	4-4.5 hr	np	8/8 +++

Summarizes data of 58 experimental neonatal and 12 sham control rats based on 6 experiments. It presents the number, age and time when the rats were sampled after inoculation with a hyphae-phase strain of *C. albicans*. Histopathology = tissue lesions with/without inflammatory cell infiltrates or the presence of yeast cells and/or hyphae in liver (l), kidney (k) and spleen (s). Not observed = negative, not performed = np. Meningitis was recorded as either a minimal numbers of neutrophils within the leptomeningeal blood vessels associated with the leptomeninges = +/-, or remarkably high numbers of leukocytes, primarily neutrophils observed within the leptomeningeal veins and post-capillary venules, cerebral cortex and/or brain ventricles = +++ with/without hemorrhage and tissue necrosis. p.o = by mouth; i.n. = intranasal; i.p. = intraperitoneal; i.c. = intracerebral.

C. albicans histopathology and the BBB

liver and spleen, while the lung tissue was negative for hyphae and leukocytic infiltrates. The liver pathology included inflammatory foci that were composed of mixed leukocytes (data not shown). Brain inflammation consisted of a limited numbers of neutrophils in association with meningeal blood vessels identified in 4/22 rats inoculated i.p. (Fig. 1c, Table 1). Hyphae were occasionally observed in association with ependymal cells lining the ventricles (Figs. 1d). Intracerebral inoculations demonstrated limited evidence of brain inflammation at 1 and 3 hrs. The degree of meningeal inflammation consisted of neutrophils with hemorrhagic foci at 4-4.5 hrs after i.c. inoculation. A profound neutrophilic meningitis was observed at 4-18 hrs after i.c. inoculation. At these times the inflammatory foci and brain pathology were extensive and demonstrated numerous neutrophils and mycelia within the lateral ventricles with associated tissue necrosis of the ependymal cell layer and adjacent, deeper brain tissues (Fig. 1e).

Light microscopy and immunohistochemistry in cell culture

In the cultures infected with the hyphae-producing,

wild-type (CAI4-URA) strain, the BMVEC that were infected by hyphae, ICAM-1 was upregulated on membrane surfaces where the yeast cells were attached to or invading the BMVEC. In these EC cultures, some of the hyphae appeared to be coated with the ICAM-1 reaction product (Fig. 1f). Other BMVEC not in association with hyphae presented a normal, constitutive expression of ICAM-1 reaction product as a weak brown HRP-DAB reaction product (data not shown).

SEM

SEM studies examined the surface topography of the cell-cell interactions between both strains of *C. albicans* and the BMVEC cultures at 1 and 2 hr after infection. These studies complemented subsequent cross-sectional, TEM/HVEM views of BMVEC/*Candida* interactions. We observed that both yeast- and hyphae strains of *C. albicans* adhered to the BMVEC at 1 hr post-inoculation. Both strains became internalized by the BMVEC at 2 hrs after inoculation. The BMVEC transformed from the flat, stellate ECs (Fig. 2a) to plump, cuboidal cells (Fig. 2b-e) as a response to the infectious process. During EC invasion, the EC membrane surfaces transformed from a relatively

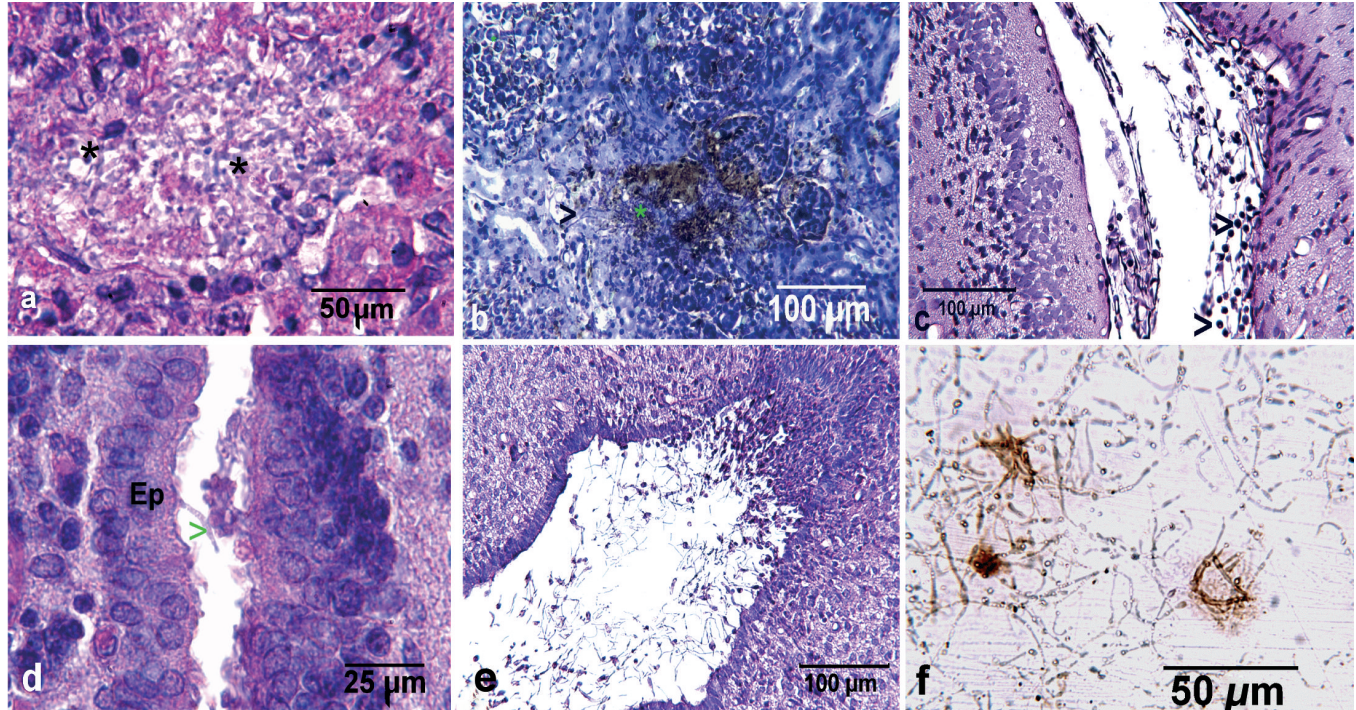


Fig. 1. Light microscopic views from 4-6 day old rats (a-e) and cell culture (f). a. Kidney cortex shows CAI4-URA mycelia (*) by H&E stain 48 hr after i.p. inoculation. b. Immunohistochemical staining of mycelia (green *) in the same animal is shown as a dark brown color in an adjacent section. c. Mild meningitis is shown in a 4 day rat 36 hr. after i.p. inoculation. Note the scattered neutrophils (>). d. H&E stain shows a single hypha (>) protruding from an ependymal cell (Ep) from the brain of an i.p.-inoculated rat pup. e. An H&E stained section shows the edge of the brain lateral ventricle in a 6 day rat 18hrs. after i.c. inoculation. Note the numerous hyphae and neutrophils at the edge of the ependymal cell layer. f. Light microscopic view of a 3 mm plastic disc shows cultured BMVEC 2 hr after inoculation with CAI4-URA. Note the strong brown-colored ICAM-1 reaction product associated with three ECs, while the filamentous hyphae not attached/invasive BMVEC express less ICAM-1 immunoreaction product.

smooth surface with few microvilli to cells containing a more rugged appearance expressing a variety of membrane microvilli, ruffles, and bleb-like extensions (Fig. 2d, e). Extended membrane ruffles (lamellopodia) appeared to embrace both blastospores (Fig. 2e) and hyphae (Fig. 3a, b).

TEM

Cross-sectional analyses of BMVEC infected after 1 and 2 hr with both strains of *C. albicans* addressed

questions concerning the process of internalization of the blastospores and hyphal forms of the yeast. Determining size differences between internalized hyphae and blastospores was often subjective. However, close inspection of the ultrastructure of the ECs containing both hyphae and blastospores are depicted in Figs. 3d-f. These figures demonstrate the smaller cross-sectional diameters or oblique views that likely represent hyphae (ca. 2 μm in diameter), while the larger compartmentalized sphere-like structures represent blastospores (ca. 5 μm in diameter). Immuno-

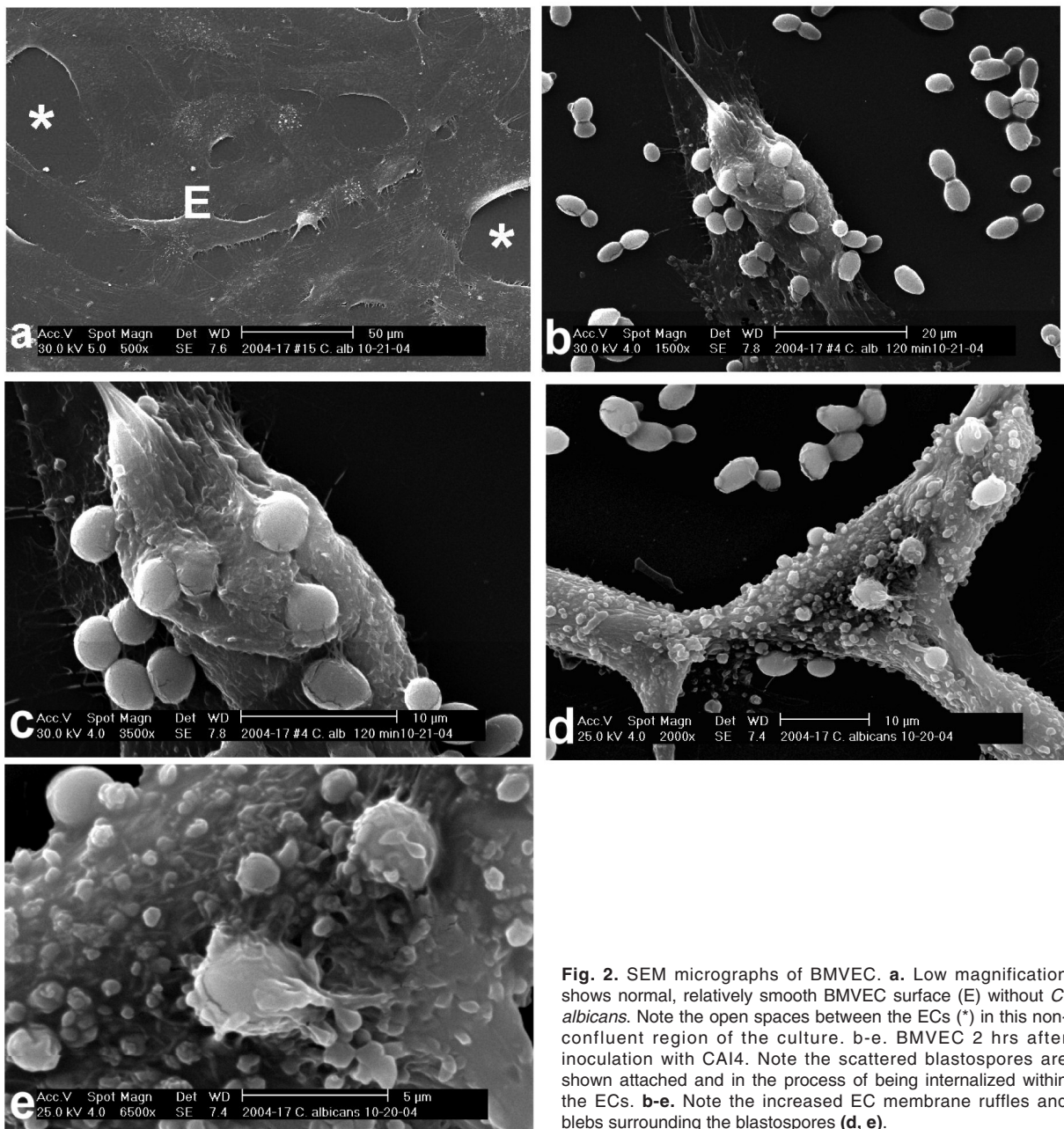


Fig. 2. SEM micrographs of BMVEC. **a.** Low magnification shows normal, relatively smooth BMVEC surface (E) without *C. albicans*. Note the open spaces between the ECs (*) in this non-confluent region of the culture. **b-e.** BMVEC 2 hrs after inoculation with CA14. Note the scattered blastospores are shown attached and in the process of being internalized within the ECs. **b-e.** Note the increased EC membrane ruffles and blebs surrounding the blastospores (**d, e**).

C. albicans histopathology and the BBB

ultrastructural studies of ICAM-1-reacted BMVEC after 1 and 2 hr infection of either strain of *C. albicans* indicated that this adhesion molecule upregulated primarily on the EC apical surfaces and within internal caveolae (Fig. 3g), on microvilli on the apical EC surfaces (Fig. 3h), and within the inner delimiting

membrane surfaces of the vacuoles that contained either blastospores or hyphae (Fig. 3i).

HVEM

In order to further assess internal aspects of *C.*

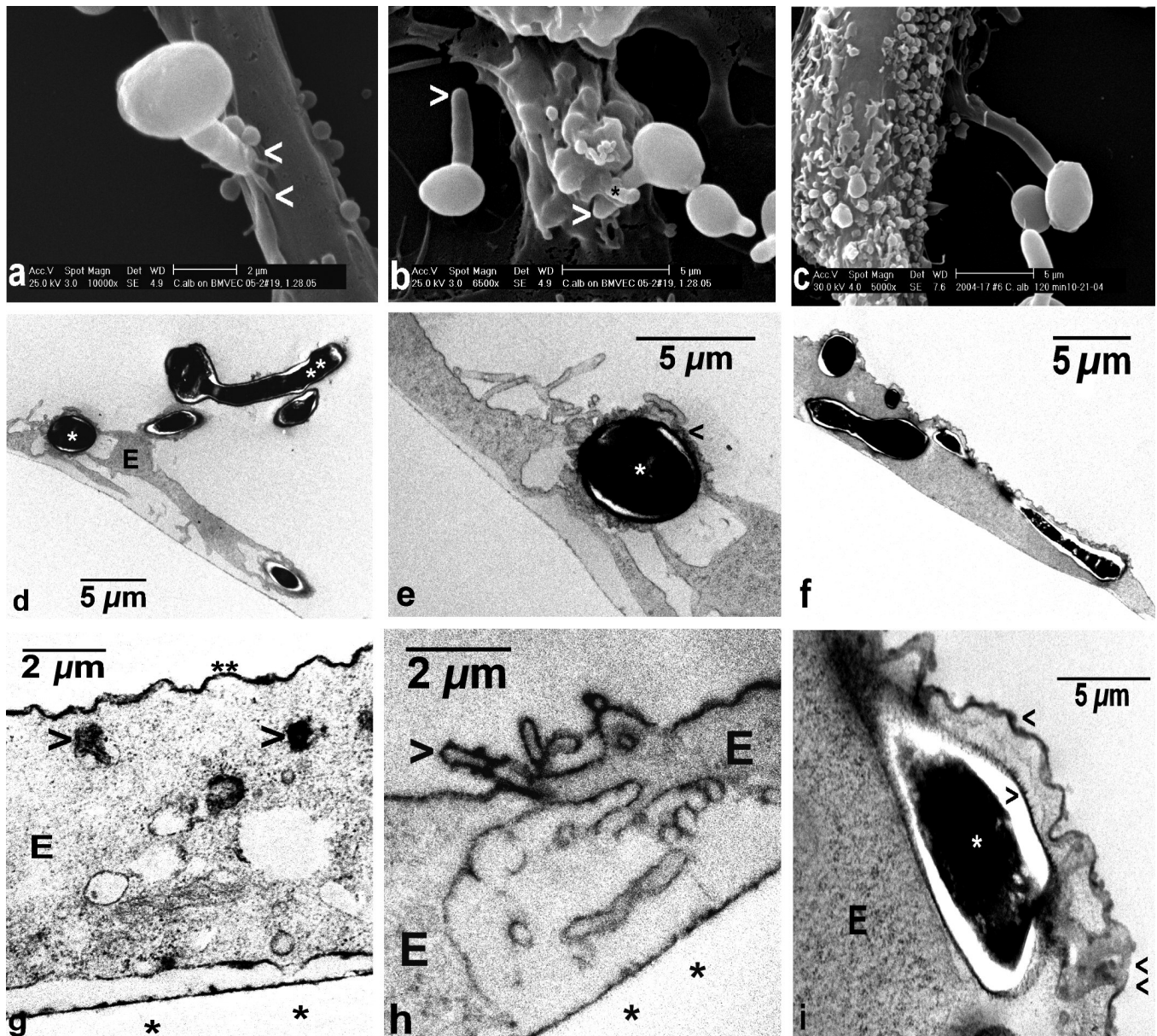


Fig. 3.a-c. SEMs show germ tubes (a, b) and an elongated hypha (c) 1hr after infection with CA14-URA. Note the EC microvilli and membrane ruffles (< in a, * in b) enveloping the germ tubes (> in b). c. Rough EC surface blebs and ruffles come into contact with the tip of an advancing hypha. **d-f.** TEM images 2 hr after inoculation with CA14-URA shows blastospores enveloped by BMVEC (d, e) and internalization of hyphae in d, f. Note the difference in the cross-sectional diameters between the blastospore (ca. 5 μ m) and the budding hypha (ca. 2-3 μ m) in the top portion of d. **g-i.** TEM images 2 hr after inoculation with either CA14 or CA14-URA show increased ICAM-1 reaction product shown as a black electron dense, HRP-DAB material on the luminal EC surfaces (g-i), on the abluminal EC surface and within modified caveolae (g), and on microvilli in (h). i. A section of a hypha is internalized within a large vacuole (a modified vesiculo-vacuolar organelle) shows ICAM-1 decorating the inner delimiting membrane surface (>), on the apical surface of the EC (<), and staining a structure that appears to represent a conduit extending between the vacuole containing the hypha to the outside of the EC (double <).

albicans CA14-URA within BMVEC, plastic thick-sections were examined by high-voltage TEM using a tilt-stage goniometer. This approach enabled us to compare BMVEC after exposure to the wild-type, hyphae-phase organisms. Because HVEM studies evaluate ten-fold thicker sections compared to thin-

sections studied by conventional TEM, we could observe numerous hyphae in the process of adhering to and invading BMVEC (Fig. 4a). We also tilted the specimen stage at slight angles on either side of the horizontal sectional plane to give a greater depth of field as observed in stereo-pair images. This enabled one to

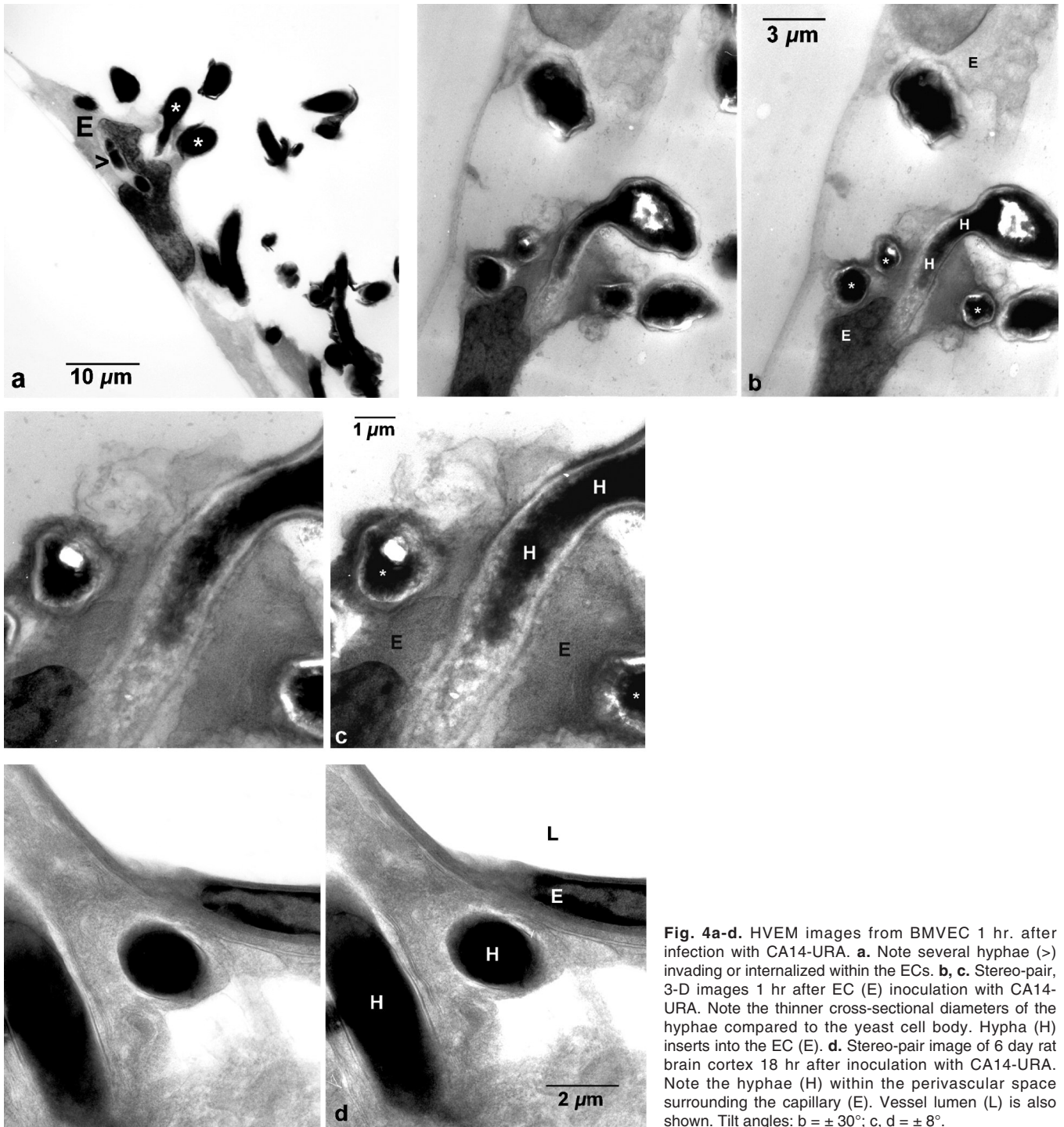


Fig. 4a-d. HVEM images from BMVEC 1 hr. after infection with CA14-URA. **a.** Note several hyphae (>) invading or internalized within the ECs. **b, c.** Stereo-pair, 3-D images 1 hr after EC (E) inoculation with CA14-URA. Note the thinner cross-sectional diameters of the hyphae compared to the yeast cell body. Hypha (H) inserts into the EC (E). **d.** Stereo-pair image of 6 day rat brain cortex 18 hr after inoculation with CA14-URA. Note the hyphae (H) within the perivascular space surrounding the capillary (E). Vessel lumen (L) is also shown. Tilt angles: b = ± 30°; c, d = ± 8°.

C. albicans histopathology and the BBB

visualize the hyphae in 3-dimension (3-D) in the process of invading the BMVEC, directly into the cytoplasm of the ECs (Fig. 4b, c). In rats that received i.c. inoculations of CAI4-URA, the fungal hyphae were often observed in 3-D within the cortical perivascular space (Fig. 4d).

Discussion

Tissue pathology in neonatal rats

In order to explore the invasive characteristics of *C. albicans*, we initially used LM to examine tissue pathology in neonatal rats. Histologic results depicted several features of the invasive characteristics of *C. albicans*. Results demonstrated that the severity of tissue pathology and meningitis produced in neonatal rat pups is related to the route of inoculation and the type of *C. albicans* inoculated. Injecting an active, hyphae-producing strain of *C. albicans* into either the peritoneum, the nose and the mouth produced limited tissue pathology within the brain meninges (exclusively the i.p. route), and within local nasal tissues, visceral organs and abdominal muscles (i.n. and i.p. routes respectively). Lung tissue did not present pathology with either stains of *C. albicans*. As shown in Table 1, pathologic lesions produced by i.p. inoculations were observed primarily in the kidneys, with less inflammation in the liver, spleen, gut and the brain meninges. Intracerebral yeast inoculation, however, produced the most dramatic meningitis within a time span we studied (4-18 hrs post inoculation), with lesser amounts of tissue inflammation and hemorrhage at 1 and 3 hrs after inoculation. These observations suggest that after i.p. inoculation (4/22 rats), some of the yeast invaded the systemic circulation and reached the brain leptomeninges while the most active meningitis in neonatal rats was produced by direct exposure of the brain and meninges to the hyphae-producing yeast strain between 4-18 hrs after inoculation (16/16 rats).

Rodents have served as good experimental models to study the microvasculature of the BBB during brain development (Bradbury, 1979; Lossinsky et al., 1986; Stewart and Hayakama, 1994; Stolp et al., 2005). Development of the immature BBB in the fetus and newborn, like that of the immune system of the developmental CNS is thought to proceed at a sluggish pace, an impediment that may have serious implications with respect to infection (Levy, 2005). This is germane to pathologic and potentially fatal conditions in premature infants including neonatal meningitis, in which pathogenic microorganisms are more capable of entering an immunologically and structurally insufficient BBB (Davis and Rudd, 1994; Lossinsky and Shivers, 2004). Thus, better understanding the structural and immunologic maturation processes of the BBB as it develops and matures is of critical importance in human, neonatal medicine. Meningitis was produced by i.p. inoculations with the hyphae-producing strain of *C. albicans* presented here in 4/22 rat pups (Table 1). While these results were limited, they may reflect the immature

nature and increased leakiness of the neonatal rat BBB. Since the neonatal BBB is structurally incomplete during the first two weeks after birth in mice (Lossinsky et al., 1986) and in rats (Ohsugi et al., 1992), we presume that the hyphae-producing strain of *C. albicans* penetrated the systemic circulation via thin-walled venous blood vessels in the mesentery and eventually entered the systemic circulation, the leptomeninges and CNS compartments. Meningoencephalitis was produced only after the fungus breached the capillaries of the BBB (Moylet, 2003, Fig. 1c, d). The other model of producing meningitis was by inoculating the fungus directly into the brain (Fig. 1e). Thus, some of the active yeast was exposed to the meningitis where it produced meningoencephalitis.

Our studies demonstrated tissue pathology was produced by i.p. inoculations of a hyphae-producing strain of *C. albicans*, (CAI4-URA). Since *C. albicans* is an autotrophic organism, it has a limited ability to proliferate within the host tissues. During the process of tissue infection, *C. albicans* transforms from the unicellular, blastospore stage and begins to form germ tubes, pseudohyphae and true filamentous hyphae (Phan et al., 2000; Brown, 2002), depending upon environmental conditions (Saville et al., 2003). The yeast to hyphal transition (dimorphism) (Korting et al., 2003) is usually considered to be the most important criterion for virulence of *C. albicans* (Naglik et al., 2003). Hyphae-phase forms of yeasts express thigmotropism, i.e., the phenomenon by which hyphae extend outward towards rough surfaces and penetrate pores (Gow, 1997; Watts et al., 1998). Thus, the hyphae were capable of locating and penetrating the kidneys, liver and other organs, as well as membrane crevices and openings on the vasculature wall, such as the loosely connected adventitial layer, vascular basement membrane and fenestrated or continuous-type EC junctional complexes. Thus, increased hyphal penetration of the thin-walled veins and post-capillary venules from either the luminal or abluminal aspects of the vasculature would appear more likely compared to the cellular or blastospore forms of the fungus that may not express aggressive movement towards rough surfaces. We speculate here that once the hyphal forms entered the systemic circulation, fungemia resulted. The hyphae subsequently made contact with the luminal EC surfaces of the less-restrictive developing meningeal blood vessels, likely became phagocytized by the EC membrane ruffles (Figs. 2e, 3e,i) and entered the modified vesiculo-vacuolar organelles (VVOs). Once internalized within the EC vacuoles, they continued their journey across the BBB.

Our light microscopic data also indicate that inoculating CAI4-URA strain of *C. albicans* via nasal and oral routes did not produce tissue pathology or meningitis. Further, the most profound form of meningitis and brain pathology was produced by the intracerebral route of inoculation. The olfactory pathway has been considered as an alternative pathway to the brain, by circumventing the restrictive BBB (Balin et al.,

1986; Illum 2004). It has been shown in experimental animals that the olfactory pathway can permit passage of various substances into the brain including proteins (Balin et al., 1986), various drugs (Bergstrom et al., 2002; Minn et al., 2002), and encephal meningitis has been produced via the olfactory pathway by viruses (Feuer et al., 2003). Thus, one would expect brain infection by *C. albicans* via the nose, as was presented above (Davis and Rudd, 1994). Although *C. albicans* is a normal inhabitant of the intestinal tract, fungi usually enter the brain following fungemia after entering the body via a vascular catheter or across the gut (Del Brutto, 2000; Holler et al., 2004).

Meningitis produced by fungi including aspergillosis, blastomycosis, candidosis, cryptococcosis and others (Del Brutto, 2000) has been observed in immunocompromised individuals (Casada et al., 1997; Levy, 2005) and in patients in hospitals (Reusser et al., 1989; Liu et al., 2003). There is, however, no evidence in the literature that *C. albicans* produces meningitis in healthy individuals. Although *C. albicans* is commonly present within the normal flora of the nasal mucosa, neither *C. albicans* fungemia nor meningitis was found in a study of nursing students with extended hospital training periods (Bonassoli and Svidzinski, 2002). Thus, it appears unlikely that *Candida* meningitis will progress via the olfactory pathway in healthy adult humans. Between 4-6 day neonatal rats (Table 1) with developing immune systems did not develop meningitis via the olfactory pathway after i.n. inoculations. This may reflect the mother's efficiency in cleaning away the yeast, an inadequate dose of the active yeast used in our experiments, a species affect or other and remains unclear. Table 1 also suggests that we could not produce meningitis after oral inoculation. Recent studies have addressed the issue of gastric fungemia produced by gastric inoculation of *C. albicans* (Yamaguchi et al., 2005). These authors studied the gastric and fecal yeast contents in mice fed various purified and commercial diets. Because higher numbers of yeast were found in the feces of mice fed a commercial diet compared to mice fed with a purified diet, it was thought that the fungus was likely suppressed by organic acids produced by lactobacilli. Since mother's milk contains high lactobacillus content, early establishment of the gut microflora as a result of immediate nursing may interfere with the production of gastric candidiasis. Thus, it is possible that the gut microflora in our 4-6 day nursing neonatal rats may have been established enough to prevent gastric fungemia. Similar to the above explanation for the i.n. rats, the paucity of induced tissue pathology in the neonatal rats examined here by the oral route may also relate to an inadequate dose of the inoculum, species differences or other affects.

C. albicans invasion of BMVEC

To further understand the adhesion and invasive mechanisms of *C. albicans* in the BBB, we performed ultrastructural and immunoultrastructural studies of

BMVEC infected with both strains of *C. albicans*. Ultrastructural data presented here describe adhesion and invasion of both yeast- and hyphae-producing strains of *C. albicans* by BMVEC. Topographic and cross-sectional views of the yeast-EC interaction demonstrated that both blastospores and hyphae adhered to the surface of BMVEC and became internalized within BMVEC between 1 and 2 hrs after inoculation. Some fungal cells were attached to rough-surfaced EC membranes, many of which produced increased microvilli. HVEM examinations of 10-fold thicker sections compared to conventional TEM thin-sections enabled us to examine the nature of invasion of the hyphae into the ECs in BMVEC and perivascularly *in vivo* by stereo-pair, 3-D images. Results suggest that both blastospores (Figs. 2b-e, 3e) and hyphae (Fig. 3d,f) were engulfed by the BMVEC. The hyphae may have actively invaded the BMVEC as they probed the surface for an entrance (Figs. 3a-c, 4a-c). It is also possible that the blastospores shown in Fig. 2b-e may have their hyphae already internalized and hidden from view by SEM. This is reasonable if one compares the SEM micrograph in Fig. 2c to the image produced by HVEM in Fig. 4b.

The phagocytic capabilities of ECs have been well documented. Normal hepatic sinusoidal ECs have been shown to express phagocytic characteristics (Lossinsky and Wisniewski, 1986; Lossinsky and Shivers, 2004), and inflammatory leukocytes are known to be engulfed by brain CNS-type ECs in experimental autoimmune conditions (Lossinsky et al., 1989a, 1991; Raine et al., 1990). The process whereby one cell is engulfed and compartmentalized by another cell and it moves about within the cell then exits the cell is called emperipolesis (Aström et al., 1968). ECs can also phagocytize bacteria, and mycotic organisms (Filler et al., 1995; Zink et al., 1996; Huang et al., 2000; Huang and Jong, 2001). We have suggested that the internalization process of cells by ECs is linked to the modification of caveolae during the inflammatory process (Liu et al., 2002; Lossinsky and Shivers, 2004). Vesiculo-vacuolar organelles (VVOs) are essentially modified caveolae that have been identified in ECs in experimental models of neoplasia (Dvorak et al., 1996) and in the altered ECs in human brain tumors (reviewed in Lossinsky et al., 1999). There is building evidence suggesting that the VVOs may serve as important conduits through which inflammatory cells and assorted pathogens traverse several blood-tissue barriers including the BBB (Lossinsky and Shivers, 2004).

ICAM-1 is a key adhesion molecule that facilitates leukocyte-endothelial adhesion and transcellular migration (Rothlein et al., 1986; Kishimoto and Rothlein, 1994), and it has been implicated in the internalization process of HIV-1 virus via modified caveolae (Liu et al., 2002). This adhesion molecule is also linked to the inflammatory process produced by *C. albicans* *in vivo* (Cannom et al., 2002). ICAM-1 has been shown to be induced directly by *C. albicans* (Orozco et al., 2000), and *C. albicans*-infected HUVEC upregulated ICAM-1 and the pro-inflammatory cytokine

C. albicans histopathology and the BBB

IL-8, leading to recruitment of activated neutrophils to the site of fungal infection (Filler et al., 1996). Blocking ICAM-1 using antibodies produced against this adhesion molecule inhibited both *C. albicans* adherence to human oral epithelial cells and the production of IL-8. These studies emphasized the importance of ICAM-1 in modulating the expression of IL-8 after fungal infection (Egusa et al., 2005).

ICAM-1 upregulates within membrane caveolae and VVOs in ECs during inflammatory events (Lossinsky et al., 1999; Lossinsky and Shivers, 2004), and increased ICAM-1 localizes in modified caveolae and macropinosomes in HIV-1-infected BMVEC (Liu et al., 2002). Immunoultrastructural data presented here demonstrate increased expression of ICAM-1 within modified EC caveolae and larger vesicular and vacuolar structures, on the apical and basal plasmalemmal surface membranes, on EC microvilli and fronds, and also decorating the inner delimiting membrane surfaces of large vacuoles containing hyphae and blastospores (Fig. 3g-i). Based on these data, similar to its influence on inflammatory leukocytes, upregulated ICAM-1 molecules likely play an important role in EC-Candida interactions. Thus, we speculate that ICAM-1 may modulate transmigration of *C. albicans* via a transcellular pathway composed of modified caveolae and VVOs in BMVEC. That the inner delimiting membrane surfaces of these VVOs and vacuoles in BMVEC containing the yeast cells and hyphae in the present studies were decorated with the reaction product for ICAM-1 (Fig. 3i) further supports the notion that the fungi were internalized within EC cellular compartments while EC junctional compartments were not involved.

Increased microvilli and fronds are thought to represent a response by the ECs to injury and inflammation (Kumar et al., 1987; Raine et al., 1990; Lossinsky et al., 1995). These membrane extensions are known to be rich in vascular cell adhesion molecule-1 (VCAM-1) (Wong and Dorovini-Zis, 1995), ICAM-1 (Lossinsky et al., 1999) and several other adhesion molecules (Carman et al., 2003). Their increased presence after EC injury, facilitate cell-cell adhesion (Lossinsky and Shivers, 2004). If one assumes that the rough surface texture of the ECs become expressed after fungus-EC adhesion in culture, the increased surface components of the ECs such as membrane microvilli and blebs observed in the present study may contribute to activation of thigmotropism and facilitate contact between the hyphae and the irregular EC surfaces (Gow, 1997; Watts et al., 1998). According to previous ultrastructural studies, modified EC caveolae in concert with adhesion molecules including ICAM-1 and others orchestrate homing of inflammatory cells to specific sites on post-capillary venules (Lossinsky et al., 1999, reviewed in Lossinsky and Shivers, 2004), facilitating invasion of the fungal hyphae via a path of less resistance. This is reasonable given that previous ultrastructural studies showed that *C. albicans* traverses HUVEC (Filler et al., 1995), aortic ECs (Zink et al.,

1996) and human brain ECs (Jong et al., 2001) via a transcellular, endocytic pathway. The yeast cells and hyphae were observed to be initially embraced by upregulated ICAM-1-positive endothelial cell fronds and ruffles, then presumably transported across BMVEC via a transcellular pathway, rather than a paracellular route. Here, in BBB-type human brain EC cultures, we provide immunoultrastructural evidence that the hyphae and blastospores became shrouded with ICAM-1 as they entered the ECs in culture. We suggest here that the process of thigmotropism may direct the hyphae into openings of the exoplasmic membrane composed of ICAM-1-positive VVOs on the luminal surface. Which of these events occurs initially remains unclear. Taken together, our observations suggest that the hyphae and blastospores were internalized by non-junctional, membrane compartments that represent a transcellular rather than paracellular transport pathway. Since cytoplasmic membranes are involved in the EC internalization process, it is likely that ICAM-1 plays an important role in modulating fungal trafficking into and across BMVEC, as has been discussed above.

Collectively, the results indicate that the modified ICAM-1-labeled EC caveolae and vacuoles were derived from the luminal EC plasma membranes and represent a continuum of the inward invagination of the luminal EC membranes, that eventually surround and compartmentalized the yeast and their hyphae (Lossinsky et al., 1999; Lossinsky and Shivers, 2004). Whether or not *C. albicans* may negotiate the BBB *in vivo* using a transcellular mechanism similar to that described here for BMVEC, its transport that may be influenced by EC junctional adhesion molecules (Schenkel et al., 2002; Muller, 2003), or its transmigration across the BBB may involve some Trojan leukocyte carrier cell(s) is unclear and further study will be required for clarification. We believe that the present report is the first description to demonstrate yeast-EC interaction in a model of the BBB using a combination of SEM, TEM and high-voltage TEM in conjunction with immunoultrastructural techniques. These kinds of comparative studies will enable us to formulate appropriate questions to address in future studies that may lead to the development of novel therapeutic interventions.

Acknowledgements. This work was supported by: 1) The Huntington Medical Research Institutes, 2) a grant from the National Institutes of Allergy and Infectious Diseases RO3 AI055636-01, -02, and 3) The Wadsworth Center's Resource for Visualization of Biological Complexity, (Albany, NY) which is supported by grant RR01219 from the National Center for Research Resources of the National Institutes of Health. This work was presented in part at the Society for Neuroscience, San Diego, CA, October, 2004 and Washington, D.C., November, 2005. We thank Mr. Clarence Graham and Mr. Jesus Chavez for technical support with histology and electron microscopy respectively and Drs. Scott G. Filler and Douglas McCreery for their critical review of the manuscript.

References

- Aström K.E., Webster H.F. and Arnason B.G., A. (1968). The initial lesion in experimental allergic neuritis. A phase and electron microscopic study. *J. Exp. Med.* 128, 469-495.
- Baer J. (2004). California Institute of Technology, Pasadena, CA, personal communication.
- Balin B.J., Broadwell R.D., Salzman M. and el-Kalliny M. (1986). Avenues for entry of peripherally administered protein to the central nervous system in mouse, rat and squirrel monkey. *J. Comp. Neurol.* 2, 260-280.
- Bergstrom U., Franzen A., Eriksson C., Lindh C. and Brittebo E.B. (2002). Drug targeting to the brain: transfer of picolinic acid along the olfactory pathways. *J. Drug Target* 10, 469-478.
- Bonassolli L.A. and Svidzinski T. (2002). Influence of the hospital environment on yeast colonization in nursing students. *Med. Mycol.* 40, 311-313.
- Bradbury M. (1979). The blood-brain barrier during the development of the individual and the evolution of the phylum. In: *The concept of a blood-brain barrier*. Bradbury M. (ed). John Wiley & Sons. New York. pp 289-322.
- Bray D.F., Bagu J. and Koegler P. (1993). Comparison of hexamethyldisilazane (HMDS), peldri II, and critical-point drying methods for scanning electron microscopy of biological specimens. *Microsc. Res. Tech.* 26, 489-495.
- Brown A.J.P. (2002). Morphogenesis signaling pathways in *Candida albicans*. In: *Candida and candidiasis*. Caldron R.A. (ed). ASM. Press. Washington, D.C. pp 95-106.
- Cannom R.R.M., French S.W., Johnston D., Edwards Jr. J.E. and Filler S.G. (2002). *Candida albicans* stimulates local expression of leukocyte adhesion molecules and cytokines in vivo. *J. Infect. Dis.* 186, 389-396.
- Carman C.V., Jun C.-D., Salas A. and Springer T.A. (2003). Endothelial cells proactively form microvilli-like membrane projections upon intercellular adhesion molecule 1 engagement of Leukocyte LFA-1. *J. Immunol.* 171, 6135-6144.
- Casada J.L., Quareda C., Oliva J., Navas E., Moreno A., Pintado V., Cobo J. and Corral I. (1997). Candidal meningitis in HIV-1-infected patients: analysis of 14 cases. *Clin. Infect. Dis.* 25, 673-676.
- Chimelli L. and Mahler-Araujo M.B. (1997). Fungal infections. *Brain Pathol.* 7, 613-627.
- Davis P.A. and Rudd P.T. (1994). Neonatal meningitis. McKeith Press. London. pp 1-177.
- Del Brutto O.H. (2000). Central nervous mycotic infections. *Rev. Neurol.* 30, 447-459.
- Dvorak A. M., Kohn S., Morgan E.S., Fox P., Nagy J. A. and Dvorak H.F. (1996). The vesiculo-vacuolar organelle (VVO): a distinct endothelial cell structure that provides a transcellular pathway for macromolecular extravasation. *J. Leuk. Biol.* 59, 100-115.
- Egusa H., Nikawa H., Makihiro S., Jewett A., Yatani H. and Hamada T. (2005). Intercellular adhesion molecule 1-dependent activation of interleukin 8 expression in *Candida albicans*-infected human gingival epithelial cells. *Infect. Immun.* 73, 622-626.
- Feuer R., Mena I., Pagarigan R.R., Harkins S., Hassett D.E. and Whitton J.L. (2003). Coxsackievirus B3 and the neonatal CNS: the roles of stem cells, developing neurons, and apoptosis in infection. *Am. J. Pathol.* 163, 1379-1393.
- Filler S.G., Pfunder A.S., Spellberg B.J., Spellberg J.P. and Edwards Jr., J.E. (1996). *Candida albicans* stimulates cytokine production and leukocyte adhesion molecule expression by endothelial cells. *Infect. Immun.* 64, 2609-2617.
- Filler S.G., Swerdloff J.N., Hobbs C. and Luckett P.M. (1995). Penetration and damage of endothelial cells by *Candida albicans*. *Infect. Immun.* 63, 976-983.
- Gow N.A. (1997). Germ tube growth of *Candida albicans*. *Curr. Top. Med. Mycol.* 8, 43-55.
- Haudenschild C.C., Cotran R.S., Gimbrone Jr., M.A. and Folkman J. (1975). Fine structure of vascular endothelium in culture. *J. Ultrastruct. Res.* 50, 22-32.
- Hayat M.A. (1981). Staining. In: *Principles and techniques of electron microscopy. Biological applications*. Vol. 1. Hayat M.A. (ed). Academic Press. New York. pp 241-318.
- Holler B.S., Omar S.A., Farid M.D. and Patterson M.J. (2004). Effects of fluid and electrolyte management on amphotericin B-induced nephrotoxicity among extremely low birth weight infants. *Pediatrics* 113, e608-e616.
- Huang S.-H. and Jong A. (2001). Cellular mechanisms of microbial proteins contributing to invasion of the blood-brain barrier. *Cell Microbiol.* 3, 277-287.
- Huang S.-H., Stins M.F. and Kim K.S. (2000). Bacterial penetration across the blood-brain barrier during the development of neonatal meningitis. *Review. Microbes. Infect.* 2, 1237-1244.
- Illum L. (2004). Is nose-to-brain transport of drugs in man a reality? *J. Pharm. Pharmacol.* 56, 3-17.
- Jong A.Y., Stins M.F., Huang S.-H., Chen S.M., and Kim K.S. (2001). Traversal of *Candida albicans* across human blood-brain barrier *in vitro*. *Infect. Immun.* 69, 4536-4544.
- Kalimo H., Garcia J.H., Kamiyo Y., Tanaka J., Valigorsky J.M., Jones R.T., Kim K.M., Mergner W.J., Pendergrass, R.E. and Trump B.F. (1974). Cellular and subcellular alterations of human CNS. Studies utilizing in situ perfusion fixation at immediate autopsy. *Arch. Pathol.* 97, 352-359.
- Karnovsky M.J. (1965). A formaldehyde-glutaraldehyde fixative of high osmolarity for use in electron microscopy. *J. Cell Biol.* 27, 137A.
- Kishimoto T.K. and Rothlein R. (1994). Integrins, ICAMs and selectins: Role and regulation of adhesion molecules in neutrophil recruitment to inflammatory sites. *Adv. Pharmacol.* 25, 117-169.
- Korting H.C., Hube B., Oberbauer S., Januschke E., Hamm G., Albrecht A., Borelli C. and Schaller M. (2003). Reduced expression of hyphal-independent *Candida albicans* proteinase genes SAP1 and SAP3 in the *egf1* mutant is associated with attenuated virulence during infection of oral epithelium. *J. Med. Microbiol.* 52, 623-632.
- Kumar K., White B., Kraus G., Garritano A.M. and Koestner A. (1987). Cerebral endothelium microvilli following global brain ischemia in dogs. *Brain Res.* 421,309-314.
- Levy O. (2005). Innate immunity of the human newborn: distinct cytokine responses to LPS and other toll-like receptor agonists. *J. Endotoxin Res.* 11, 113-116.
- Lima C. and Vital J.P. (1994). Olfactory pathways in three patients with cryptococcal meningitis and acquired immune deficiency syndrome. *J. Neurol. Sci.* 123, 195-199.
- Linscott W.D. (1999). Linscott's Directory of Immunological and Biological Reagents. In W.D. Linscott. Santa Rosa. pp 1-378.
- Liu N.Q., Lossinsky A.S., Popik W., Li X., Gujuluva C., Kriederman B., Roberts J., Pushkarsky T., Bukrinsky M., Witte M., Weinand M. and Fiala M. (2002). Human immunodeficiency virus type 1 enters brain microvascular endothelia by macropinocytosis dependent on lipid rafts and mitogen-activated protein kinase signaling pathway. *J.*

C. albicans histopathology and the BBB

- Viol. 76, 6689-6700.
- Liu Z.Y., Sheng R.Y., Li X.L., Li T.S. and Wang A.X. (2003). Nosocomial fungal infections, analysis of 149 cases. *Zhonghua Yi. Xue. Za. Zhi.* 83, 399-402.
- Lossinsky A.S. and Shivers R.R. (2003). Studies of cerebral endothelium by scanning and high-voltage electron microscopy. In: *The blood-brain barrier: Biology and research protocols.* N.S. (ed). Human Press. Totowa, N.J. pp. 67-82.
- Lossinsky A.S. and Shivers R.R. (2004). Structural pathways for macromolecular and cellular transport across the blood-brain barrier during inflammatory conditions. A Review. *Histol. Histopathol.* 19, 535-564.
- Lossinsky A.S. and Wisniewski H.M. (1986). A comparative ultrastructural study of endothelial cell tubular structures from injured mouse blood-brain barrier and normal hepatic sinusoids demonstrated after perfusion fixation with osmium tetroxide. *Microvasc. Res.* 31, 333-344.
- Lossinsky A.S., Vorbrodt A.W. and Wisniewski H.M. (1986). Characterization of endothelial cell transport in the developing mouse blood-brain barrier. *Develop. Neurosci.* 8, 61-75.
- Lossinsky A.S., Badmajew V., Robson J., Moretz R.C. and Wisniewski H.M. (1989a). Sites of egress of inflammatory cells and horseradish peroxidase transport in a murine model of chronic relapsing experimental allergic encephalomyelitis. *Acta Neuropathol.* 78, 359-371.
- Lossinsky A.S., Song M.J. and Wisniewski H.M. (1989b). High-voltage electron microscopic studies of endothelial tubular structures in mouse blood-brain barrier following brain trauma. *Acta Neuropathol.* 77, 480-488.
- Lossinsky A.S., Pluta R., Song M.J., Badmajew V., Moretz R.C. and Wisniewski H.M. (1991). Mechanisms of inflammatory cell attachment in chronic relapsing experimental allergic encephalomyelitis. A scanning and high-voltage electron microscopic study of the injured mouse blood-brain barrier. *Microvasc. Res.* 41, 299-310.
- Lossinsky A.S., Vorbrodt A.W. and Wisniewski H.M. (1995). Scanning and transmission electron microscopic studies of microvascular pathology in the osmotically impaired blood-brain barrier. *J. Neurocytol.* 24, 795-806.
- Lossinsky A.S., Buttle B.F., Pluta R., Mossakowski M.J. and Wisniewski H.M. (1999). Immunoultrastructural expression of intercellular adhesion molecule-1 in endothelial cell vesiculo-tubular structures and vesiculo-vacuolar organelles in blood-brain barrier development and injury. *Cell Tissue Res.* 295, 77-88.
- Minn A., Leclerc S., Heydel J.M., Minn A.L., Denizcot C., Cattarelli M., Netter P. and Gradinaru D. (2002). Drug delivery into the mammalian brain: the nasal pathway and its specific metabolic barrier. *J. Drug Target.* 10, 285-296.
- Moylet E.H. (2003). Neonatal *Candida* meningitis. *Semin Ped. Infec. Dis.* 14, 115-122.
- Muller W.A. (2003). Leukocyte-endothelial-cell interactions in leukocyte transmigration and the inflammatory response. *Trends Immunol.* 24, 326-333.
- Naglik J.R., Challacombe S.J. and Hube B. (2003). *Candida albicans* secreted aspartyl proteinases in virulence and pathogenesis. *Microbiol. Molec. Biol. Revs.* 67, 400-428.
- Ohsugi M., Sato H. and Yamamura H. (1992). Transfer of 125I-albumin from blood to brain in newborn rats and the effect of hyperbilirinemia on the transfer. *Biol. Neonate* 62, 47-54.
- Orozco A.S., Zhou X. and Filler S.G. (2000). Mechanisms of the proinflammatory response of endothelial cells to *Candida albicans* infection. *Infec. Immun.* 68, 1134-1141.
- Phan Q.T., Belanger P.H. and Filler S.G. (2000). Role of hyphal formation in interactions of *Candida albicans* with endothelial cells. *Infec. Immun.* 68, 3485-3490.
- Raine C.S., Cannella B., Duijvestijn A.M. and Cross A.H. (1990). Homing to central nervous system vasculature by antigen-specific lymphocytes. II. Lymphocyte/endothelial cell adhesion during the initial stages of autoimmune demyelination. *Lab. Invest.* 63, 476-489.
- Reusser P., Zimmerli W., Scheidegger D., Marbet G.A., Buser M. and Gyr K. (1989). Role of gastric colonization in nosocomial infections and endotoxemia: a prospective study in neurosurgical patients on mechanical ventilation. *J. Infec. Dis.* 160, 414-421.
- Rothlein R., Dustin M.L., Marlin S.D. and Springer T.A. (1986). A human intercellular adhesion molecule (ICAM-1) distinct from LFA-1. *J. Immunol.* 137, 1270-1274.
- Saville S.P., Lazzell A.L., Monteagudo C. and Lopez-Ribot J.L. (2003). Engineered control of cell morphology *in vivo* reveals distinct roles for yeast and filamentous forms of *Candida albicans* during infection. *Eukaryot. Cell* 2, 1033-1060.
- Schenkel A.R., Mamdouh Z., Chen X., Liebman R.M. and Muller W.A. (2002). CD99 plays a major role in the migration of monocytes through endothelial junctions. *Nature Immunol.* 3, 143-150.
- Shi S.-R., Key M.E. and Karla K.L. (1991). Antigen retrieval in formalin fixed paraffin-embedded tissue: An enhancement method for immunohistochemical staining based on microwave oven heating of tissue sections. *J. Histochem. Cytochem.* 39, 741-748.
- Stewart P.A. and Hayakawa K. (1994). Early ultrastructural changes in blood-brain barrier vessels of the rat embryo. *Dev. Brain Res.* 78, 25-34.
- Stolp H.B., Dziegielewska K.M., Ek C.J., Habgood M.D., Lane M.A., Potter A.M. and Saunders, N.R. (2005). Breakdown of the blood-brain barrier to proteins in white matter of the developing brain following systemic inflammation. *Cell Tissue Res.* 320, 369-378.
- Watts H.J., Véry A.-A., Perera T.H.S., Davies J.M. and Gow N.A.R. (1998). Thigmotropism and stretch-activated channels in the pathogenic fungus *Candida albicans*. *Microbiology* 144, 689-695.
- Witek-Janusek L., Shareef M.J. and Mathews H.L. (2002). Reduced lymphocyte-mediated antifungal capacity in high-risk infants. *J. Infec. Dis.* 186, 129-133.
- Wong D. and Dorovini-Zis K. (1995). Expression of vascular cell adhesion molecule-1 (VCAM-1) by human brain microvessel endothelial cells in primary culture. *Microvasc. Res.* 49, 325-339.
- Yamaguchi N., Sonoyama K., Kikuchi H., Nagura T., Aritsuka T. and Kawaba J. (2005). Gastric colonization of *Candida albicans* differs in mice fed commercial and purified diets. *J. Nutr.* 135, 109-115.
- Zink S., Nass T., Rosen P. and Ernst J.F. (1996). Migration of the fungal pathogen *Candida albicans* across endothelial monolayers. *Infec. Immun.* 64, 5085-5091.